

A Supervised Machine Learning Approach for Accelerating the Design of Particulate Composites: Application to Thermal Conductivity

Mohammad Saber Hashemi¹, Masoud Safdari², Azadeh Sheidaei^{1*}

¹ Aerospace Engineering Department, Iowa State University, Ames, IA 50011, United States

² Aerospace Engineering Department, University of Illinois, Urbana-Champaign 61820, USA

Abstract

In this paper, we present a supervised machine learning (ML) based computational framework for designing particulate multifunctional composite materials for desired thermal conductivity (TC). In this framework, the design variables are physical descriptors of the material microstructure to link microstructure to properties for material design. The design of experiment (DoE) based on Sobol sequence was utilized to generate a sufficiently large database for training ML models accurately. Microstructures were realized through an efficient, fast packing algorithm, and the TC of microstructures were obtained using our previous Fast Fourier Transform (FFT) homogenization method. Thereafter, the ML methods constituting a reduced-order model (ROM) was trained over the generated database to establish the complex relationship between the structure and properties. Finally, the ROM is used for material design through an optimization algorithm to solve the inverse problem of finding the material with desired properties represented by its physical descriptors. The results showed that the surrogate model is accurate in predicting the behavior of microstructure with respect to high-fidelity FFT simulations, and inverse design is robust in finding microstructure parameters according to case studies.

Keywords: Multifunctional Particulate Composite, Machine Learning, Thermal Conductivity, Genetic Algorithm, Material Design, Structure-Property Relation

1. Introduction

Computational material design (CMD), an emerging field of study, is a strong technique in material design and developing advanced multifunctional materials []. Accomplishing the goal of these studies depends on the appropriate representation of the material microstructure as the design variables. Microstructure characterization and reconstruction (MCR) techniques, which are generally considered to represent the microstructure, can be categorized into (1) Correlation function-based methods [1–4], (2) Physical descriptor-based methods [5–7], (3) Spectral density

Corresponding author: Azadeh Sheidaei, PhD

Aerospace Engineering Department, Iowa State University, Ames, IA 50011, United States

Tel: [515-294-2956](tel:515-294-2956) (O)/Fax: [515-294-3262](tel:515-294-3262) (O)

Email: Sheidaei@iastate.edu

function-based characterization and reconstruction by level-cutting a random field [8] or by disk-packing [9], (4) Unsupervised ML-based methods such as convolutional deep neural networks [10] and instance-based learning [11] as well as supervised ML ones such as encoding and decoding the microstructure through Markov random field [12], and (5) Texture synthesis-based methods [13,14] based on the review study of Bostanabad et al. [15] and recent studies using deep learning methods. Categories 1, 4, and 5 cannot be used for material design since they do not provide us with specific design variables. Others may involve some dimensional reduction due to high-dimensional representations, which should be cautiously studied to avoid significant information loss, which decreases the structural variability. As an effort to address this problem, Yang et al. [16] have presented a deep adversarial learning methodology generative to train generative adversarial networks (GANs) for mapping between low-dimensional latent variables (design variables) and microstructures. They have also used the Bayesian optimization framework to obtain microstructures with the desired material property. All in all, the most convenient yet capable category for material design is the physical descriptor-based methods.

Bessa et al. [17] have proposed a framework for data-driven analysis of materials under uncertainty to facilitate the modelling and design of new material systems. Their framework consists of DoE, efficient creation of a material response database (Data Generation), and using ML methods to find some response model or a new material design. However, they cited high-fidelity analyses at a low computational cost as the main hurdle in data generation phase when analyses are inherently complex, e.g. 3D analyses of heterogenous representative volume elements (RVEs) under irreversible deformation, or there is a high dimensional design space requiring too many sample points to be evaluated. In order to accelerate the data generation phase, ROMs could be utilized instead of direct time-consuming numerical simulations. For instance, Liu et al. [18] have developed a self-consistent clustering analysis (SCA) as an ROM with accurate predictions in irreversible processes. Other examples of ROMs are micromechanics-based methods [19,20], the transformation field analysis (TFA) [21], the nonuniform transformation field analysis (NTFA) [22], the principal component analysis [23] also known as proper orthogonal decomposition (POD) [24], and the proper generalized decomposition (PGD) [25].

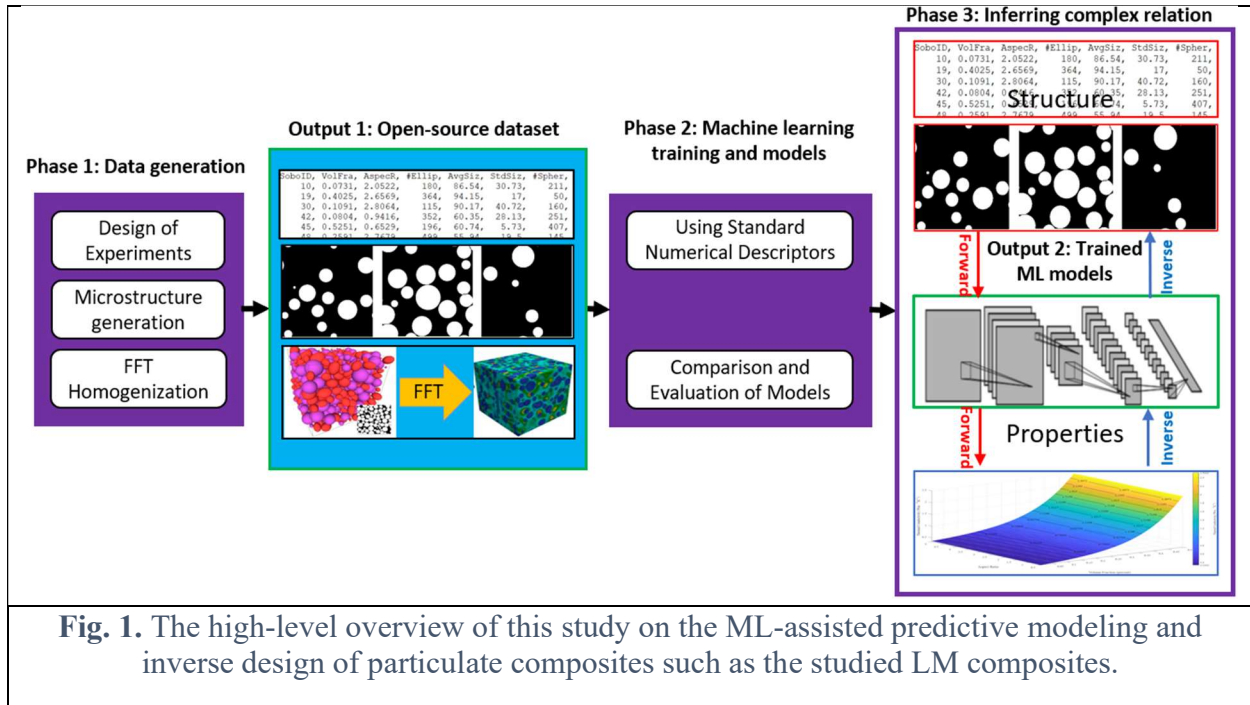
The multifunctional particulate composite material studied in this paper is Liquid Metal (LM) elastomer. LM composites constitute a new class of multifunctional materials with concurrent electrical, TC, and mechanical compliance, which has multiple potential applications in areas such as wearable devices, electronics, robotics, and biomedical. Over the past few years, research progress on LM composites was in methods to synthesize LM droplets and their suspension within various matrix materials. Currently, material scientists are working on developing methods that can precisely control the average size (Avg), size distribution, and yield of LM droplets with a wide variety of surfactants, polymer coatings, and dispersion media [26–31]. As these methods are further refined, there will be an increasing need for computational tools that aid in designing LM composites with target material properties. The determination of the effective properties of

composite materials given their specific constituents has been widely explored in the past decades. High-fidelity FE simulations of the response of composite materials yield accurate predictions, but the associated computational time limits their applicability in the design phase.

In this study, we developed a computational framework to obtain accurate and inexpensive predictions of the TC of LM composites as well as to understand their dependence on the microstructural geometry based on optimal ML algorithms. To have a sufficiently large dataset for advanced supervised and unsupervised ML algorithms, we cannot only rely on the experimental results of the material. Even best designed experimental procedures cannot cover all feature vectors required for the ML training as diverse as their computational counterparts. Therefore, a robust and efficient design scheme of virtual experiments, i.e., computational simulations, was necessary to have a representative sample of the random variables affecting the performance of a trained ML model. First, we focused on generating an open-source labeled dataset which was sufficiently large and representative for the training of supervised learners. Second, we tried to discover the complex relationship between the structure and properties using ML. The direct problem of finding the effective properties of a material system given its microstructure parameters, such as volume fraction (VF) and size distribution was addressed using a deep neural network optimized given the available dataset. The inverse problem of material design, i.e., finding microstructure parameters given its properties as inputs, was solved using a gradient-based optimization method. The trained network with high prediction accuracies acted as the robust surrogate model of the objective function. Virtual experiments based on the optimization results demonstrate the ability of our proposed framework for the material design of particulate composites.

2. Method

The overview of the material discovery framework is shown in [Fig. 1](#). The high-level overview of this study on the ML-assisted predictive modeling and inverse design of particulate composites such as the studied LM composites.. Phase 1, data generation, was necessary to train machine learners over a labeled dataset. Phase 2 involved finding the complex relationship between the structure and properties using appropriate ML algorithms. The first objective was finding the effective properties of a material system given its microstructure parameters, such as VF, size distribution, and aspect ratio (AR). The second objective was inverse design, i.e., finding microstructure parameters given its properties as inputs. The microstructure could be realized, given its parameters or 3-D visualization through computational packing algorithms in the studied material system. Thus, Phase 3 was inferring and visualizing of the forward structure-property relationships as well as generating microstructures from the inverse design framework.



2.1. Data Generation

A greater dataset size would lead to better predictive models due to more accurate estimation of the probabilistic dependencies among the system random variables. To have a sufficiently large dataset for advanced ML algorithms, we cannot only rely on the experimental results of the material. Even best designed experimental procedures cannot cover all feature vectors, material system characteristics in this study, required for the ML training as diverse and representative as their computational counterparts. Therefore, a robust and efficient design scheme of virtual experiments, i.e., computational simulations, was necessary to have a representative dataset of the random variables, which were the microstructure physical descriptors in this study, affecting the performance of a trained ML predictive model. The output of this phase is an open source dataset which could open new horizons for research on material discovery, especially when it can be applied to similar material systems of particulate composites with different material constituents.

2.1.1. Design of Experiment

The target variables to be predicted are those of an effective TC tensor of a particulate composite given a specified set of materials for the composite constituents. The properties will be computationally measured using a homogenization technique. Since the TC is governed by linear Laplacian equation, and the material coefficients of the constituents were assumed to be constant with respect to the temperature, a set of constant boundary conditions can be prescribed based on the homogenization technique. Thus, the only remaining parameters which affect the property are the microstructure morphology. Since the studied particulate composite was insulated or non-percolated LM elastomer, the type of material characterization and microstructure reconstruction

we chose was based on the physical descriptors [15]. Subsequently, the method of microstructure reconstruction was particle packing [32]. It has been shown in previous studies [26–31] that the shape of LM particles are ellipsoidal with varying ARs, and there is a particle size distribution which can be parametrized by a normal or Gaussian curve given a set of average and standard deviation parameters. To account for different ARs, two ARs for particles were considered: 1 for spherical particles, and a number other than one for all other ellipsoidal particles. Fig. 2. (a) a gaussian distribution curve with an average parameter of 0 and a standard deviation σ . (b) an ellipsoidal shape with semi-axes a , b , and c . For this study, it is assumed that two of them are always equal, so that the last one can be determined by the above formula with an AR number. shows the definition of the latter number, and an example of a gaussian distribution function. Another important geometrical factor in composites is the VF of the constituents. The physical descriptors and their bounds as well as the numbers of particles, which are necessary for packing algorithm performance, are summarized in

Table 1. $VF(\%)$ is the volume fraction of LM particles, AR is the AR of ellipsoidal particles, $Avg(\mu m)$ is the average LM particle size, $Std(\mu m)$ is the standard deviation of the particle sizes, $\#Ell$ is the number of ellipsoidal particles, and $\#Sph$ is the number of spherical particles. The bounds of variables were selected based on an experimental work [29].

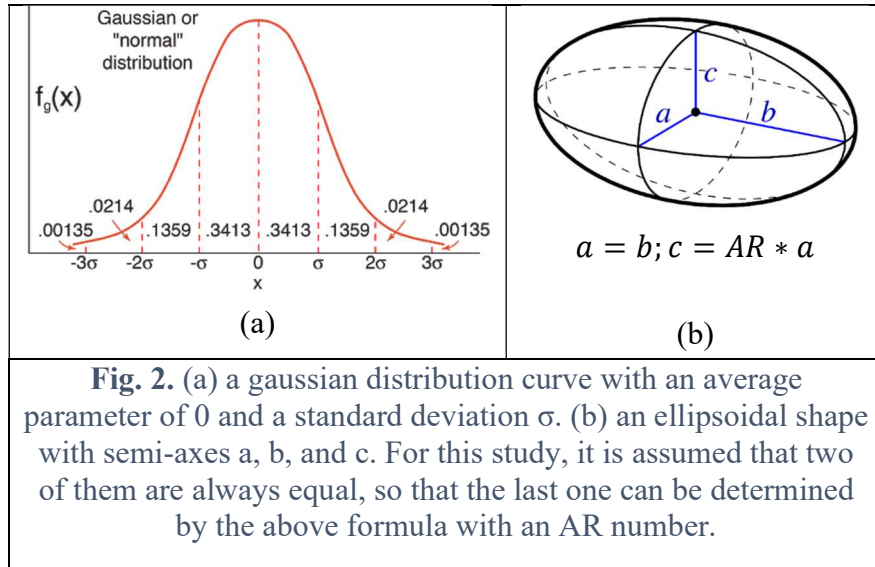


Table 1. The bounds on the physical descriptors of the microstructure as well as the numbers of particles inside a pack.

	$VF(\%)$	AR	$\#Ell$	$Avg(\mu m)$	$Std(\mu m)$	$\#Sph$
Lower Bounds	1	0.5	1	0.1	0.1	1
Upper Bounds	60	3.0	500	100.0	100.0	500

After identifying and limiting the microstructure parameters affecting the properties, a method of DoE was used to explore the design or input variables' domain for training machine learners or fitting different metamodels efficiently. Since there was no prior knowledge of the conditional probabilities of the microstructural inputs and the property output, and each microstructure variable was considered equally important in determining the material properties, space-filling designs which equally cover different regions of the design space were chosen. Two constraints on space-filling designs are even spread of points to be used for computational experiment inside the experimental region and avoiding replication when the points are projected in different subsets of design or input variables or the so-called non-collapsing condition [33]. Santiago et al. [34] have indicated that different optimum Latin Hypercube Samplings [35] and the Sobol sequence [36], a deterministic low discrepancy sequence, show a better balance between more regular distribution or randomness while being closer to a regular grid or better coverage of the input variables space. Thus, we chose the Sobol sequence, which is also very fast in generating the experiment points.

2.1.2. Microstructure Generation

Rocpack code [37] was used to generate a microstructure for each point of DoE. This new packing code is a derivative of the Lubachevsky-Stillinger (LS) algorithm [32] for packing disks and spheres, in which a set of infinitesimally small particles gradually grow while undergoing elastic collisions to avoid intersection. The algorithm is called event-based since the simulation of particle collisions evolves from an event or collision to another one instead of fixed time steps. This process was not efficient due to time-consuming collision detection. Therefore, the new code addressed the problem by growing the infinitesimal particle points in their places, not randomly shooting them in the space, until they are close to overlapping each other, in which case Monte Carlo trial displacements replaced the classic elastic collisions. The code is also compatible with the material characterization presented in section 2.1.1. In other words, each pack of particles as a composite microstructure can be generated with the above parameters. However, the randomness in microstructures is also present in the packing algorithm with the initial seeding, so that we can get multiple similar, not identical, realizations of a microstructure. Not all experiment points generated by the Sobol sequence are consistent or physically meaningful. For instance, the continuous normal size distribution of the particles would be discretized according to the total number of particles resulting in different growth rates and final sizes for the particles. The minimum and maximum sizes of particles can be consequently determined by [Eq. \(1\)](#).

$PDF(r) = \frac{1}{Std\sqrt{2\pi}} e^{-\frac{1}{2}\left(\frac{r-Avg}{Std}\right)^2} \xrightarrow{PDF=\frac{1}{N}} (r - Avg)^2 = -2Std^2 \ln\left(\frac{Std}{N}\sqrt{2\pi}\right) = Expr$	(1)
$\text{If } Expr \geq 0 \Rightarrow \begin{cases} r_{min} = Avg - \sqrt{Expr} \\ r_{max} = Avg + \sqrt{Expr} \end{cases}$	

PDF and N are the Gaussian probability distribution function and the number of particles, respectively. If the minimum size, r_{min} , is lower than zero, or $Expr$ is lower than zero, the parameters are physically inconsistent.

The numbers of particles also determine the window size or the dimension of the microstructure reconstruction in a periodic cube. This can be inferred from Eq. (2), which elucidates the implicit relationship between the physical descriptors of the microstructure.

$$\begin{aligned}
 Domain_Size &= Vol_{Total}^{\frac{1}{3}} = \left(\frac{Vol_{Inclusions}}{VF} \right)^{\frac{1}{3}} = \left(\frac{Vol_{Ellipsoids} + Vol_{Spheres}}{VF} \right)^{\frac{1}{3}} \\
 &= \left\{ \frac{1}{VF} \left(\int_{R_{min}}^{R_{max}} [4\pi * AR * r^2 * N_{Ellipsoids} * PDF(r)] dr \right. \right. \\
 &\quad \left. \left. + \int_{R_{min}}^{R_{max}} [4\pi * r^2 * N_{Spheres} * PDF(r)] dr \right) \right\}^{\frac{1}{3}}
 \end{aligned} \tag{2}$$

Packs with high VF close to the theoretical packing fraction [38] and a large diversity in particle sizes are challenging for the algorithm and computationally expensive. Therefore, packs which could not be completely generated under an hour were ignored among the whole packing inputs from the Sobol sequence results. Those packs can be generated later if improving the accuracy of the machine learners is required. The outputs of the code, i.e., 3D realization of the packs, were given as 2-D images of the sliced 3-D microstructures in one arbitrary direction due to the isotropy. Voxelization is limited by the resolution of slicing, and it cannot be arbitrarily increased since the FFT homogenization process time depends on the size of the microstructure in voxels, and we need to build a large database with the minimum computational cost. Therefore, we set the number of pixels in all directions to 300. This setting may be coarse for packs with very small LM particles and for capturing the exact geometrical shape of the particles, but it resulted in a reasonable FFT computation time, about 3 hours on average for each pack. Furthermore, the voxelization may cause some artificial defects in microstructure reconstruction when there are at least two close particles between which some voxels are marked as inclusion in slicing due to a limited resolution. This problem was resolved by applying some morphological operations and watershed filter [39] on the 2D images.

2.1.3. FFT Homogenization to Calculate Effective TC

As stated in section 2.1, the microstructure database generated according to previous steps can be used for similar material systems with different constituents. However, the material behavior and properties are also dependent on the constituent material types. Since the material of our interest was LM composites, TCs of $0.29W/mK$ and $26.4W/mK$ for the silicone elastomer matrix and eutectic gallium-indium (EGaIn) inclusions were considered. Conventional numerical methods

such as finite element (FE) for finding the effective properties of random heterogeneous material suffer from their dependency on very fine and high-quality mesh conforming to intricate geometries of phases. FFT methods were shown to be an efficient replacement when working with voxelized representative volume elements (RVEs) and no conformal meshing requirement [40]. They are also superior to other numerical methods in terms of scalability, $O(N \log N)$ in complexity vs. $O(N^3)$. We have already validated this homogenization method with the experimental results of the LM composites [41]. Reader is referred to this work for detailed discussion.

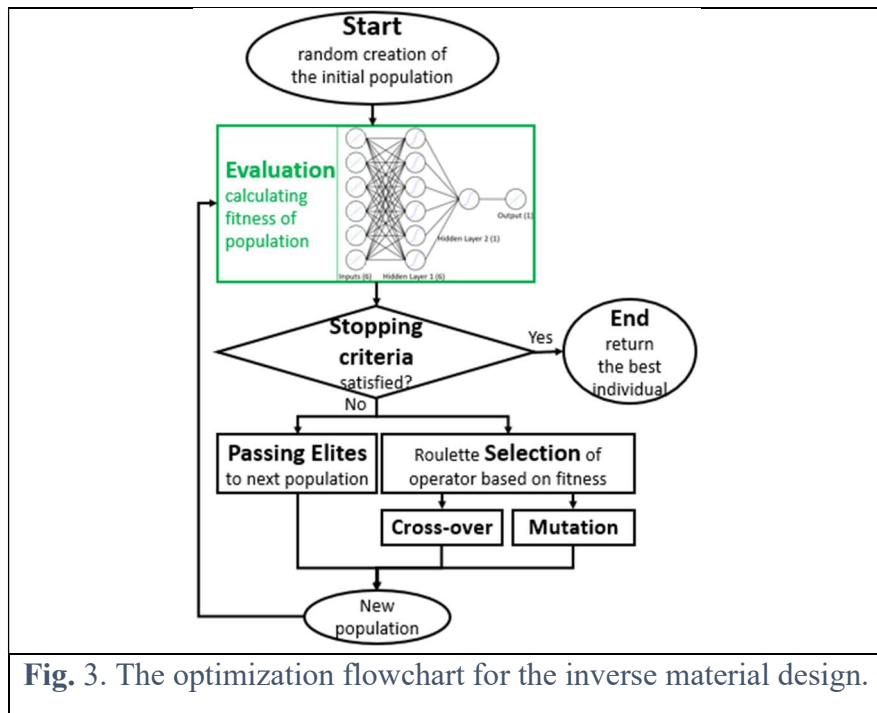
2.2. ML Training and Models

The objective of this phase was to find an efficient and optimal ML model to replace the time-consuming homogenization process. Neural networks are versatile and robust as a regression tool for modeling complex functions since each neuron can be a nonlinear function, and using different network architectures, number of neurons, number of layers, and links between neurons, may arbitrarily increase their complexity. Therefore, we considered different architectures and trained them on the dataset according to n-fold cross validation technique. The perceptron function was Sigmoid although ReLU units have been argued [] to be better when using data ranging outside the normal interval of [-1, 1]. Therefore, the input data have been linearly normalized into [-1, 1]. The inputs were vectors of physical descriptors as well as other packing parameters needed for microstructure reconstruction while the only output was the homogenized TC, which was actually the average value of the diagonal elements of the TC tensor since the studied material system was almost isotropic. The architectures grid-searched for performance optimization have been one and two fully connected layers with a range of number of neurons in each layer. The whole available dataset of homogenized packs was randomly divided into 5 equally sized sections. The neural networks were trained 5 times by using a section of data, which has not been considered previously, as a test set and the rest as a training set each time. After 5 training processes, the average training accuracy and its standard deviation were calculated so that the performance of different architectures could be compared with each other. The best performing network with the highest average training accuracy was chosen for the final training on the whole dataset.

2.3. Inferring Complex Structure-Property Relationship

So far, finding a fast and reliable ML model for material properties prediction as a surrogate of relatively expensive direct numerical solvers, FFT homogenization in this study, was explained. It establishes the direct relationship between the structure of the studied particulate material and its effective homogenized properties. However, the more demanding problem is the inverse design, i.e., what are the physical descriptors of the material system which could provide us with a set of desired effective properties. The inverse material design has been challenging due to inefficient and expensive methods of finding the material properties for a given microstructure. However, recent studies [] have tackled the problem through ROMs or surrogate models. Since our studied material system could be characterized by only 6 features or 6 physical descriptors, and we have

already established a reliable yet fast surrogate model for the direct structure-property relationship discussed in the previous sections, genetic algorithm (GA) was used to optimize the structure according to a manufacturer’s limitations on the microstructure parameters, such as VF or sizes of LM particles, to get a desired property from the material. GA is a population-based metaheuristic optimization algorithm inspired by natural selection through operators such as mutation, crossover, and selection [42]. The main prohibiting factor in evolutionary algorithms is the computational complexity due to fitness calculation of many design points in each generation or optimization iteration [43], but the objective function in our study was calculated by the trained neural network which is very fast in inference. The single target of such an optimization is the isotropic TC of the composite, and the design variables are evidently the physical descriptors considered for the microstructure characterization and reconstruction in section 2.1. Although the numbers of particles are integers, they were treated as continuous variables due to the negligible effects of their fractional parts in the surrogate model. To formulate the problem as a minimization one, the objective function was the absolute difference of the fast surrogate model prediction from the user-supplied target property. The stopping criteria of the algorithm were considered as reaching the 100th population generations (MaxGenerations), or passing 35 stall generations as an indicator of the convergence to a plateau (MaxStallGenerations), or finding one or more points in a population with an objective value equal to or lower than 0.0001 (FitnessLimit). The flowchart of the optimization method of inverse material design is shown in Fig. 3. The optimization flowchart for the inverse material design, while the evaluation step with the trained surrogate model is distinguished by green color. The GA was elitist in that a few design points or individuals with highest fitness or lowest objective function values were being passed to new populations directly.



3. Results and Discussion

3.1. Generated Database

A subset of first DoE results of almost 10000 points based on the Sobol sequence is given in [Table 2](#). The first Sobol-based inputs of the material structure database; columns 2-7 are the features of the neural network, while the last column can be calculated from them by Eq. (2).. SID is the Sobol ID or the position of the parameters in the sequence. Columns 2-7 are needed for microstructure generation. The last columns contain minimum and maximum radii of ellipsoid and spherical particles, and the domain size of the microstructure, which is required for packing algorithm, respectively. The unit of all dimensions is micrometer (μm). Naturally, Sobol IDs should be 1, 2, 3, ..., and the absent Sobol IDs are due to physically inconsistent set of parameters or others for which packs were not generated under an hour time limit as discussed in section 2.1.2.

Table 2. The first Sobol-based inputs of the material structure database; columns 2-7 are the features of the neural network, while the last column can be calculated from them by Eq. (2).

SID	VF	AR	#Ell	Avg	Std	#Sph	R_{min}^{El}	R_{max}^{El}	R_{min}^{Sph}	R_{max}^{Sph}	DS
10	7.31	2.05	180	86.54	30.73	211	46.50	126.58	42.91	130.17	866.16
19	40.25	2.65	364	94.15	17.00	50	58.94	129.36	84.54	103.76	646.36
30	10.91	2.80	115	90.17	40.72	160	70.28	110.06	51.56	128.78	602.59
42	8.04	0.94	352	60.35	28.13	251	9.91	110.79	15.52	105.18	701.15
45	52.51	0.65	196	60.74	5.73	407	47.64	73.84	45.92	75.56	360.91
48	25.91	2.76	499	55.94	19.50	145	13.91	97.97	27.18	84.70	624.58
55	31.68	1.57	393	86.49	26.17	93	36.97	136.01	64.62	108.36	585.98
56	30.29	1.88	281	83.74	1.14	87	80.29	87.19	80.76	86.72	563.29
58	5.32	1.27	295	97.35	69.93	214	26.00	168.7	53.17	141.53	971.42

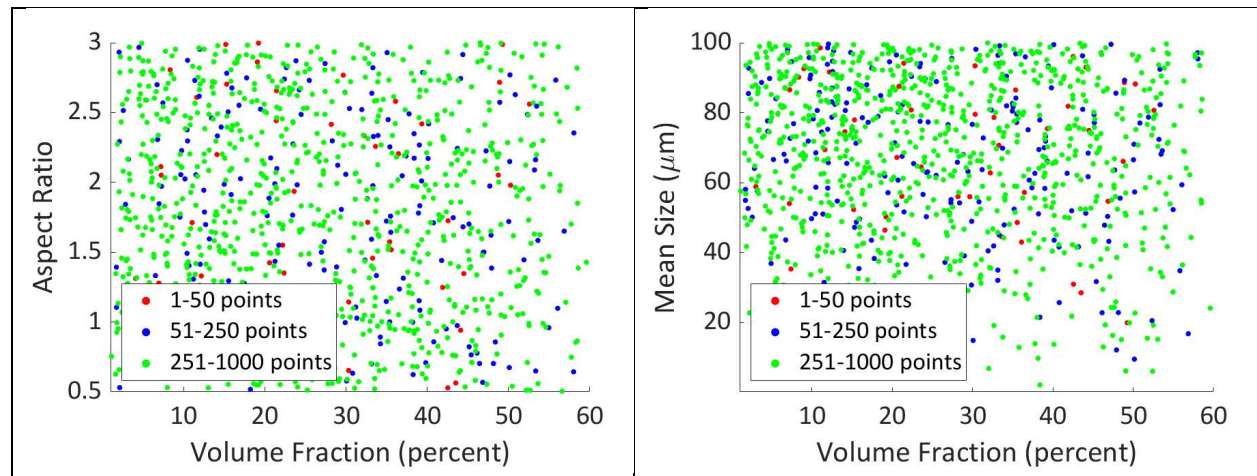


Fig. 4. The first 1000 feasible DoE points generated by the Sobol sequence projected on different 2D planes.

Space-filling designs should cover the design space almost homogeneously while they need to maintain non-collapsing constraint. From Fig. 4. The first 1000 feasible DoE points generated by the Sobol sequence projected on different 2D planes. of the generated packs, it can be inferred that the criteria are met for our Sobol DoE although some generated sets of parameters were not used in the final simulations due to physical inconsistencies or some long times needed for packing. This design has an advantage of successive coverage of space along the sequence generation, so that the dataset can be successively improved, i.e. the design space can be further explored, by continuing the previous number sequences. For instance, the first 50 DoE points of generated packs were shown by a red color, then the next 200 and the next 750 points were plotted by blue and green colors, respectively. Additionally, the projection of 6D points on different 2D planes, VF-Mean Size and VF-AR, did not overlap each other.

A sample of FFT simulation results after imposing thermal loading condition of $\Delta T=[1,0,0]$ for a set of packing parameters is shown in Fig. 5. The colorful parts of the figure illustrate the thermal gradient in different positions inside the pack, and the black-and-white sections are the images of 2D slices of the pack. The gradient is clearly larger in the regions of high concentration of particles.

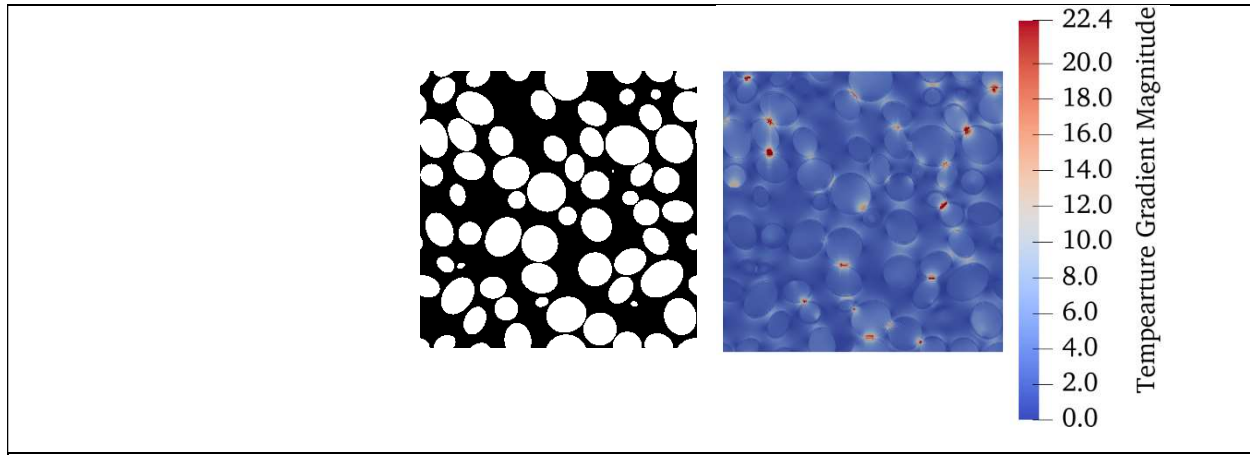


Fig. 5. The FFT simulation results of a pack under a thermal loading of $\Delta T=[1,0,0]$.

3.2. Optimized Surrogate Model of Direct Structure-Property Relationship

As stated in the method section, several network architectures were considered and trained to find an optimized network in terms of performance. Since there were six input parameters and only one output, network architectures of 3, 6, 10, 20, 50, and 100 neurons in one hidden layer for networks with one hidden layer, and 3, 6, 10, 20, 50, and 100 in the first hidden layer as well as 1, 6, 10, 20, 50, and 100 in the second hidden layer for networks with 2 hidden layers were considered. The best network was the one with highest average accuracy or lowest MSE according to cross-validation technique. The architecture is shown in Fig. 6. The optimized fully connected neural

network architecture.. After finding the optimized network, it was trained on the whole dataset. The error histogram of **Error! Reference source not found.(a)** is indicating that most errors with respect to the homogenized packs are quite small. However, the regression plot of the trained network, **Error! Reference source not found.(b)**, shows that the accuracy is lower for large conductivity composites due to less DoE points covering regions of design space with higher VFs. It is worth mentioning that the speed of the surrogate model in terms of a trained neural network is an order of 0.1 second compared with conventional method of homogenization which took an average time of 4 hours for each microstructure in our developed database.

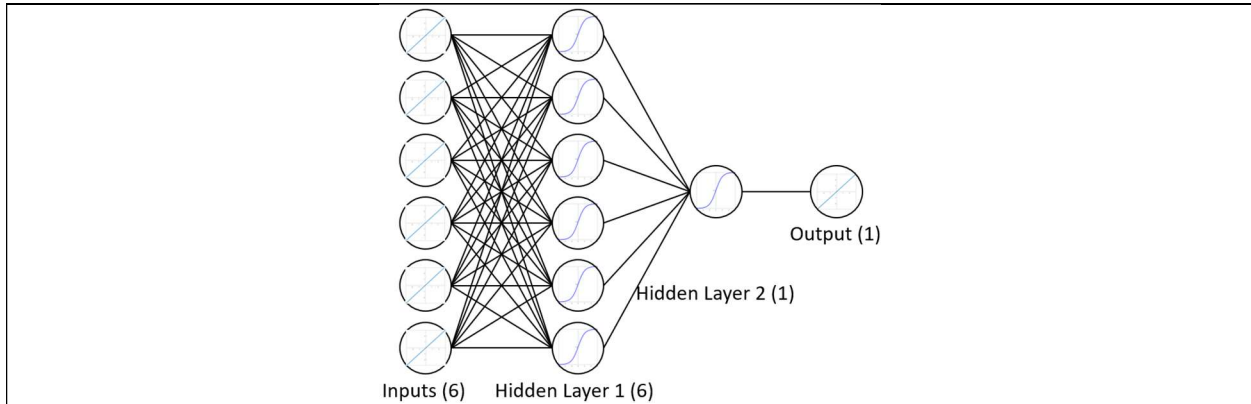


Fig. 6. The optimized fully connected neural network architecture.

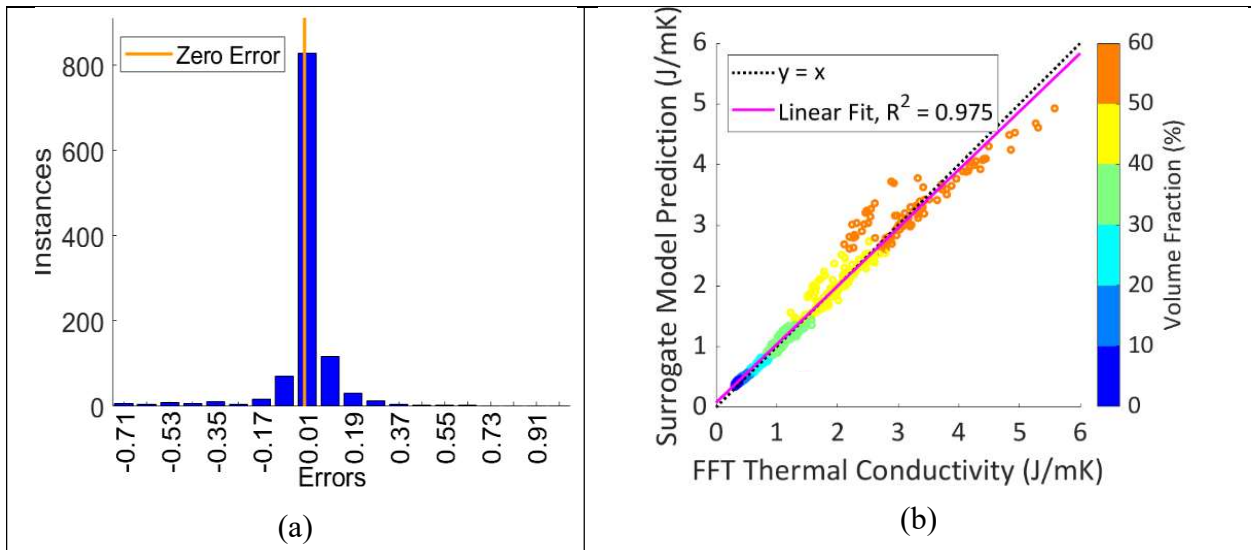


Fig. 7. (a) The error histogram of the optimized network over the whole dataset (b) regression plot of the network outputs (y-axis) vs. target values from FFT homogenization (x-axis); the colored points categorize the scatter plot into groups with different VFs.

Following our objective of inferring the direct relationship between microstructure and its properties, several response surfaces of the studied LM composite were plotted using the fast surrogate model, the trained neural network. In each surface, all microstructure features, network

inputs, were fixed except two of them, warm colors show high conductivity composites, and black lines on the surface are constant TC contours.

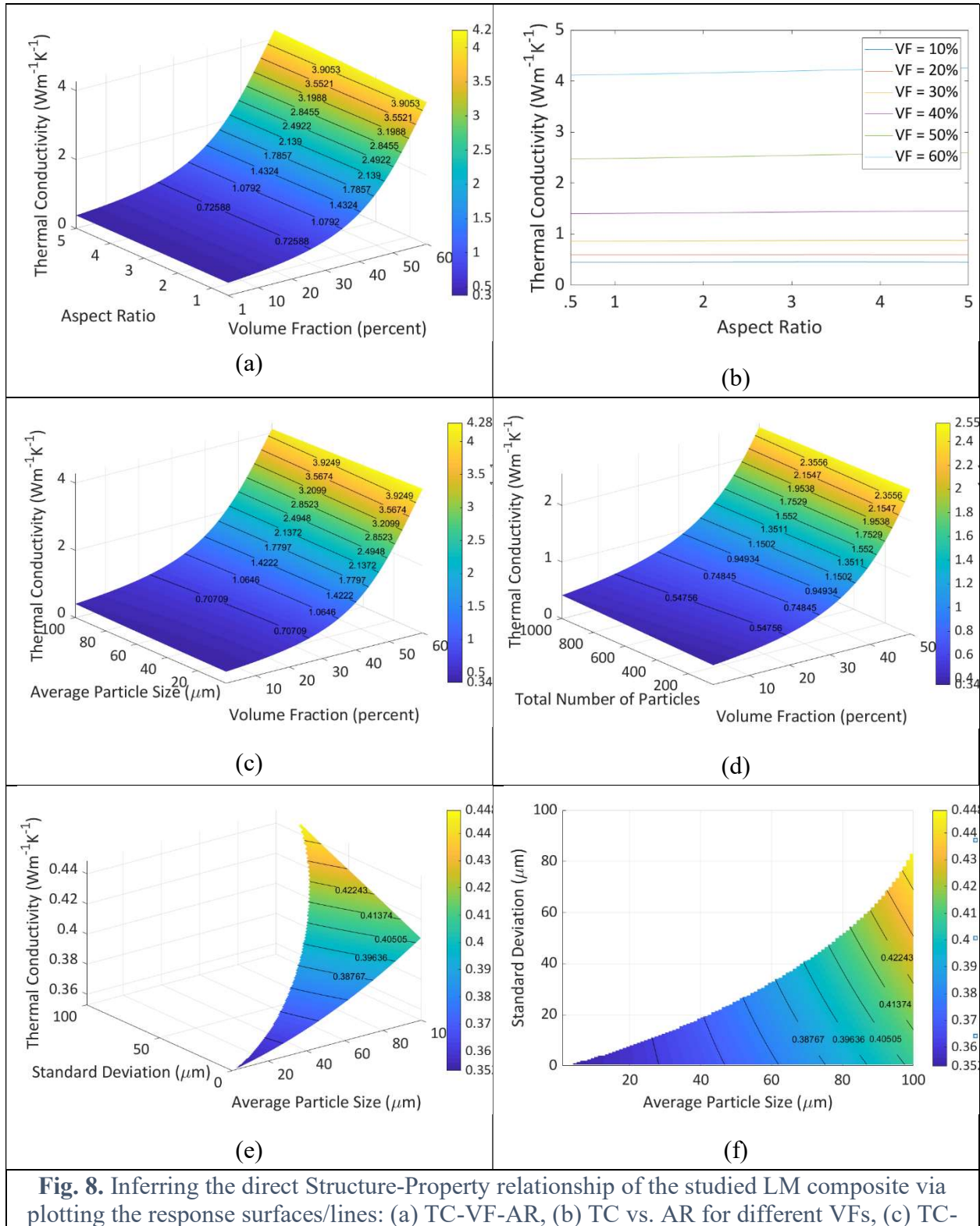
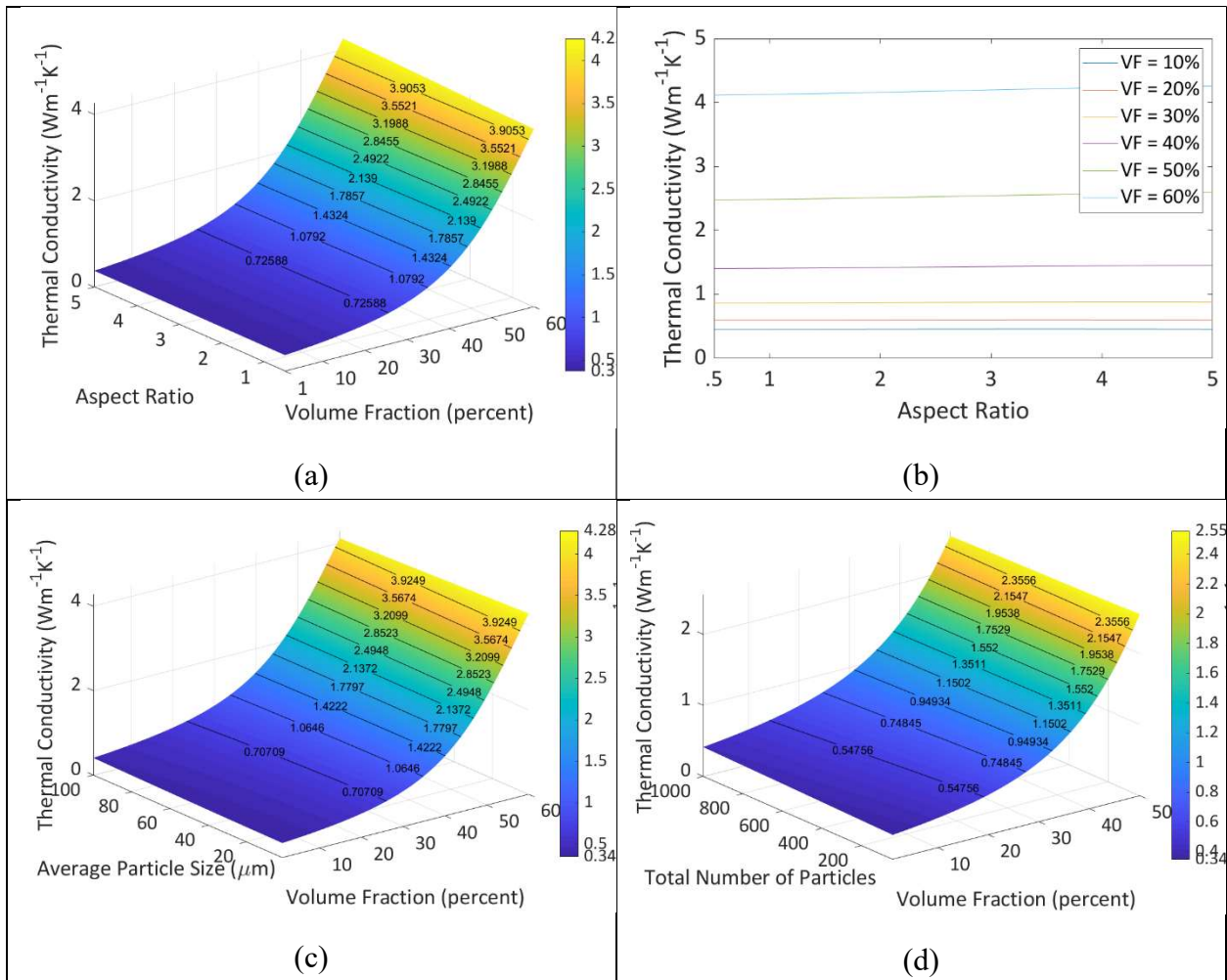


Fig. 8. Inferring the direct Structure-Property relationship of the studied LM composite via plotting the response surfaces/lines: (a) TC-VF-AR, (b) TC vs. AR for different VFs, (c) TC-

VF-Avg, (d) TC-VF-Number of Particles, (e) TC-Avg-Std, and (f) TC-Avg-Std projection on 2D plane of Avg-Std.

(a) is the response surface of TC-AR-VF. VF has the prominent effect on the property. According to Fig. 8(b), increasing AR considering a constant VF only slightly improves the TC for high VF composites, e.g. in constant 60% VF, a composite with AR of 0.5 has 4.117 TC, while TC is 4.259 for AR of 5. The effect of VF and Avg on the TC is illustrated in Fig. 8(c). Again, VF is shown to be the most important factor in TC, and the mean particle size, Avg, has a negligible effect on TC. Fig. 8(d) shows that TC has been almost constant with increasing number of particles. It is satisfactory in this study in that the standard deviation of predicted property due to the variation in microstructure size was low. In other words, the calculated domain sizes based on Eq. (2) were sufficient to define RVE sizes. Some design points are not feasible as pointed out in Eq. (1), so the projection of the TC-Avg-Std surface, Fig. 8(e), on the 2D plane of mean size and standard deviation is empty in some regions of Fig. 8(f). Thus, it can be deduced that the TC has a direct relationship with the Avg and standard deviation in particle sizes although their effects on TC are much less significant than that of VF.



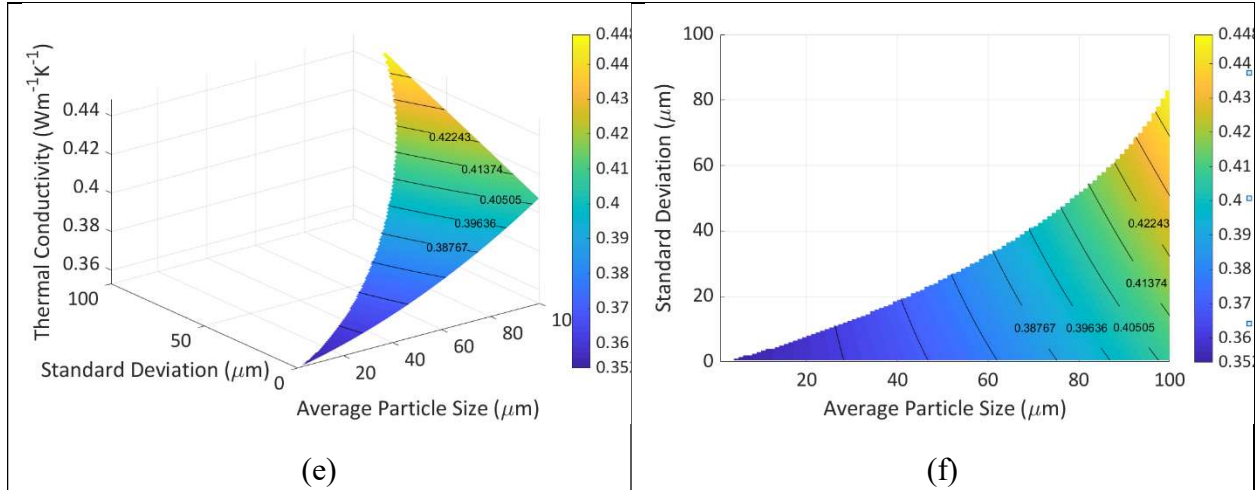


Fig. 8. Inferring the direct Structure-Property relationship of the studied LM composite via plotting the response surfaces/lines: (a) TC-VF-AR, (b) TC vs. AR for different VFs, (c) TC-VF-Avg, (d) TC-VF-Number of Particles, (e) TC-Avg-Std, and (f) TC-Avg-Std projection on 2D plane of Avg-Std.

3.3. Inverse Design via GA Optimization

A case study was done to show how our proposed method in section 2.3 works and verify its results through the data generation process discussed in section 2.1. The goal of optimization was set to 1 J/mK heat conductivity. The best design point among the last population as well as the predicted property value and the FFT calculated one are [33.5, 1.355, 161.26, 10.379, 17.08, 123.4], 0.9981, and 0.98, respectively. The number of particles were rounded to provide the packing code with valid integer numbers. Following multiple tests, such as the aforementioned case, it can be concluded that the inverse design method is efficient and accurate.

4. Conclusions

Database generation was a time-consuming yet great achievement in this research. The microstructure characteristics and reconstructions via a fast packing code can be used for similar heterogeneous particulate materials with different constituents. A surrogate ML model was trained on the database to establish the direct link between the microstructure and the conductivity property and visualize them with various response surfaces. For the studied material system, the VF is far more important in determining the conductivity; however, greater particle sizes and higher ARs slightly improves TC. The smart and physically aware choice of the specified physical descriptors for microstructure characterization and reconstruction not only provided us with less-complicated modeling of Structure-Property links with respect to the image-based convolution neural networks requiring many more training data, but also connected the results of this study directly to the process phase which is readily prepared for practical utilization by material scientists and the relevant industries. Finally, the low number of characterization features, the singularity of the objective, the target TC, and a fully connected neural network as the fast surrogate model

trained on our generated database, enabled us to use an evolutionary optimization, GA, to explore the design space and find the physical descriptors of an LM composite which will have a given TC.

References

- [1] A. Sheidaei, M. Baniassadi, M. Banu, P. Askeland, M. Pahlavanpour, N. Kuuttila, F. Pourboghrat, L.T. Drzal, H. Garmestani, 3-D microstructure reconstruction of polymer nano-composite using FIB-SEM and statistical correlation function, *Composites Science and Technology*. 80 (2013) 47–54. <https://doi.org/10.1016/j.compscitech.2013.03.001>.
- [2] S.A. Tabei, A. Sheidaei, M. Baniassadi, F. Pourboghrat, H. Garmestani, Microstructure reconstruction and homogenization of porous Ni-YSZ composites for temperature dependent properties, *Journal of Power Sources*. 235 (2013) 74–80. <https://doi.org/10.1016/j.jpowsour.2013.02.003>.
- [3] H. Amani Hamedani, M. Baniassadi, A. Sheidaei, F. Pourboghrat, Y. Rémond, M. Khaleel, H. Garmestani, Three-Dimensional Reconstruction and Microstructure Modeling of Porosity-Graded Cathode Using Focused Ion Beam and Homogenization Techniques, *Fuel Cells*. 14 (2014) 91–95. <https://doi.org/10.1002/fuce.201300170>.
- [4] C.L.Y. Yeong, S. Torquato, Reconstructing random media, *Physical Review E - Statistical Physics, Plasmas, Fluids, and Related Interdisciplinary Topics*. 57 (1998) 495–506. <https://doi.org/10.1103/PhysRevE.57.495>.
- [5] H. Xu, Y. Li, C. Brinson, W. Chen, A descriptor-based design methodology for developing heterogeneous microstructural materials system, *Journal of Mechanical Design, Transactions of the ASME*. 136 (2014). <https://doi.org/10.1115/1.4026649>.
- [6] G. Requena, G. Fiedler, B. Seiser, P. Degischer, M. di Michiel, T. Buslaps, 3D-Quantification of the distribution of continuous fibres in unidirectionally reinforced composites, *Composites Part A: Applied Science and Manufacturing*. 40 (2009) 152–163. <https://doi.org/10.1016/j.compositesa.2008.10.014>.
- [7] H. Xu, R. Liu, A. Choudhary, W. Chen, A Machine Learning-Based Design Representation Method for Designing Heterogeneous Microstructures, *Journal of Mechanical Design, Transactions of the ASME*. 137 (2015). <https://doi.org/10.1115/1.4029768>.
- [8] J.W. Cahn, Phase separation by spinodal decomposition in isotropic systems, *The Journal of Chemical Physics*. 42 (1965) 93–99. <https://doi.org/10.1063/1.1695731>.
- [9] S. Yu, Y. Zhang, C. Wang, W.K. Lee, B. Dong, T.W. Odom, C. Sun, W. Chen, Characterization and Design of Functional Quasi-Random Nanostructured Materials Using

- Spectral Density Function, *Journal of Mechanical Design*, Transactions of the ASME. 139 (2017). <https://doi.org/10.1115/1.4036582>.
- [10] R. Cang, Y. Xu, S. Chen, Y. Liu, Y. Jiao, M.Y. Ren, Microstructure Representation and Reconstruction of Heterogeneous Materials Via Deep Belief Network for Computational Material Design, *Journal of Mechanical Design*, Transactions of the ASME. 139 (2017). <https://doi.org/10.1115/1.4036649>.
- [11] V. Sundararaghavan, N. Zabarav, Classification and reconstruction of three-dimensional microstructures using support vector machines, *Computational Materials Science*. 32 (2005) 223–239. <https://doi.org/10.1016/j.commatsci.2004.07.004>.
- [12] R. Bostanabad, A.T. Bui, W. Xie, D.W. Apley, W. Chen, Stochastic microstructure characterization and reconstruction via supervised learning, *Acta Materialia*. 103 (2016) 89–102. <https://doi.org/10.1016/j.actamat.2015.09.044>.
- [13] L.Y. Wei, M. Levoy, Fast texture synthesis using tree-structured vector quantization, in: *Proceedings of the ACM SIGGRAPH Conference on Computer Graphics*, Association for Computing Machinery (ACM), New York, New York, USA, 2000: pp. 479–488. <https://doi.org/10.1145/344779.345009>.
- [14] V. Sundararaghavan, Reconstruction of three-dimensional anisotropic microstructures from two-dimensional micrographs imaged on orthogonal planes, *Integrating Materials and Manufacturing Innovation*. 3 (2014) 240–250. <https://doi.org/10.1186/s40192-014-0019-3>.
- [15] R. Bostanabad, Y. Zhang, X. Li, ... T.K.-P. in M., undefined 2018, *Computational microstructure characterization and reconstruction: Review of the state-of-the-art techniques*, Elsevier. (n.d.). https://www.sciencedirect.com/science/article/pii/S0079642518300112?casa_token=ZIs2g0pGsg0AAAAA:g4qZeUE6GajgANnWjP2SGYdSVbRMxtVhj48nX-tENjtUsv3Pn0LwIPVUcJwgeaNQdTm_8k4T (accessed July 9, 2020).
- [16] Z. Yang, X. Li, L.C. Brinson, A.N. Choudhary, W. Chen, A. Agrawal, Microstructural materials design via deep adversarial learning methodology, *Journal of Mechanical Design*, Transactions of the ASME. 140 (2018). <https://doi.org/10.1115/1.4041371>.
- [17] M.A. Bessa, R. Bostanabad, Z. Liu, A. Hu, D.W. Apley, C. Brinson, W. Chen, W.K. Liu, A framework for data-driven analysis of materials under uncertainty: Countering the curse of dimensionality, *Computer Methods in Applied Mechanics and Engineering*. 320 (2017) 633–667. <https://doi.org/10.1016/j.cma.2017.03.037>.

- [18] Z. Liu, M.A. Bessa, W.K. Liu, Self-consistent clustering analysis: An efficient multi-scale scheme for inelastic heterogeneous materials, *Computer Methods in Applied Mechanics and Engineering*. 306 (2016) 319–341. <https://doi.org/10.1016/j.cma.2016.04.004>.
- [19] J.A. Moore, R. Ma, A.G. Domel, W.K. Liu, An efficient multiscale model of damping properties for filled elastomers with complex microstructures, *Composites Part B: Engineering*. 62 (2014) 262–270. <https://doi.org/10.1016/j.compositesb.2014.03.005>.
- [20] Z. Liu, J.A. Moore, W.K. Liu, An extended micromechanics method for probing interphase properties in polymer nanocomposites, *Journal of the Mechanics and Physics of Solids*. 95 (2016) 663–680. <https://doi.org/10.1016/j.jmps.2016.05.002>.
- [21] G. Eor Ge, J.D. Vorak, Transformation field analysis of inelastic composite materials, *Proceedings of the Royal Society of London. Series A: Mathematical and Physical Sciences*. 437 (1992) 311–327. <https://doi.org/10.1098/rspa.1992.0063>.
- [22] J.C. Michel, P. Suquet, Nonuniform transformation field analysis, *International Journal of Solids and Structures*. 40 (2003) 6937–6955. [https://doi.org/10.1016/S0020-7683\(03\)00346-9](https://doi.org/10.1016/S0020-7683(03)00346-9).
- [23] I. Jolliffe, Principal Component Analysis, in: Wiley StatsRef: Statistics Reference Online, John Wiley & Sons, Ltd, Chichester, UK, 2014. <https://doi.org/10.1002/9781118445112.stat06472>.
- [24] J. Yvonnet, Q.C. He, The reduced model multiscale method (R3M) for the non-linear homogenization of hyperelastic media at finite strains, *Journal of Computational Physics*. 223 (2007) 341–368. <https://doi.org/10.1016/j.jcp.2006.09.019>.
- [25] P. Ladevèze, J.C. Passieux, D. Néron, The LATIN multiscale computational method and the Proper Generalized Decomposition, *Computer Methods in Applied Mechanics and Engineering*. 199 (2010) 1287–1296. <https://doi.org/10.1016/j.cma.2009.06.023>.
- [26] M.D. Bartlett, N. Kazem, M.J. Powell-Palm, X. Huang, W. Sun, J.A. Malen, C. Majidi, High thermal conductivity in soft elastomers with elongated liquid metal inclusions, *Proceedings of the National Academy of Sciences of the United States of America*. 114 (2017) 2143–2148. <https://doi.org/10.1073/pnas.1616377114>.
- [27] R. Tutika, S.H. Zhou, R.E. Napolitano, M.D. Bartlett, Mechanical and Functional Tradeoffs in Multiphase Liquid Metal, Solid Particle Soft Composites, *Advanced Functional Materials*. 28 (2018) 1804336. <https://doi.org/10.1002/adfm.201804336>.
- [28] C. Pan, E.J. Markvicka, M.H. Malakooti, J. Yan, L. Hu, K. Matyjaszewski, C. Majidi, A Liquid-Metal–Elastomer Nanocomposite for Stretchable Dielectric Materials, *Advanced Materials*. 31 (2019) 1900663. <https://doi.org/10.1002/adma.201900663>.

- [29] R. Tutika, S. Kmiec, A.B.M. Tahidul Haque, S.W. Martin, M.D. Bartlett, Liquid Metal-Elastomer Soft Composites with Independently Controllable and Highly Tunable Droplet Size and Volume Loading, *ACS Applied Materials and Interfaces*. 11 (2019) 17873–17883. <https://doi.org/10.1021/acsami.9b04569>.
- [30] M.H. Malakooti, N. Kazem, J. Yan, C. Pan, E.J. Markvicka, K. Matyjaszewski, C. Majidi, Liquid Metal Supercooling for Low-Temperature Thermoelectric Wearables, *Advanced Functional Materials*. 29 (2019) 1906098. <https://doi.org/10.1002/adfm.201906098>.
- [31] H. Wang, Y. Yao, Z. He, W. Rao, L. Hu, S. Chen, J. Lin, J. Gao, P. Zhang, X. Sun, X. Wang, Y. Cui, Q. Wang, S. Dong, G. Chen, J. Liu, A Highly Stretchable Liquid Metal Polymer as Reversible Transitional Insulator and Conductor, *Advanced Materials*. 31 (2019) 1901337. <https://doi.org/10.1002/adma.201901337>.
- [32] B.D. Lubachevsky, F.H. Stillinger, Geometric properties of random disk packings, *Journal of Statistical Physics*. 60 (1990) 561–583. <https://doi.org/10.1007/BF01025983>.
- [33] A. Jourdan, J. Franco, Optimal Latin hypercube designs for the Kullback-Leibler criterion, *AStA Advances in Statistical Analysis*. 94 (2010) 341–351. <https://doi.org/10.1007/s10182-010-0145-y>.
- [34] J. Santiago, M. Claeys-Bruno, M. Sergent, Construction of space-filling designs using WSP algorithm for high dimensional spaces, *Chemometrics and Intelligent Laboratory Systems*. 113 (2012) 26–31. <https://doi.org/10.1016/j.chemolab.2011.06.003>.
- [35] M.E. Johnson, L.M. Moore, D. Ylvisaker, Minimax and maximin distance designs, *Journal of Statistical Planning and Inference*. 26 (1990) 131–148. [https://doi.org/10.1016/0378-3758\(90\)90122-B](https://doi.org/10.1016/0378-3758(90)90122-B).
- [36] I.M. Sobol, Uniformly distributed sequences with an additional uniform property, *USSR Computational Mathematics and Mathematical Physics*. 16 (1976) 236–242. [https://doi.org/10.1016/0041-5553\(76\)90154-3](https://doi.org/10.1016/0041-5553(76)90154-3).
- [37] G. Amadio, T.L. Jackson, A New Packing Code for Creating Microstructures of Propellants and Explosives, in: 51st AIAA/SAE/ASEE Joint Propulsion Conference, American Institute of Aeronautics and Astronautics, Reston, Virginia, 2015. <https://doi.org/10.2514/6.2015-4098>.
- [38] F. Maggi, S. Stafford, T.L. Jackson, J. Buckmaster, Nature of packs used in propellant modeling, *Physical Review E - Statistical, Nonlinear, and Soft Matter Physics*. 77 (2008) 046107. <https://doi.org/10.1103/PhysRevE.77.046107>.
- [39] F. Meyer, Topographic distance and watershed lines, *Signal Processing*. 38 (1994) 113–125. [https://doi.org/10.1016/0165-1684\(94\)90060-4](https://doi.org/10.1016/0165-1684(94)90060-4).

- [40] H. Moulinec, P. Suquet, A numerical method for computing the overall response of nonlinear composites with complex microstructure, *Computer Methods in Applied Mechanics and Engineering*. 157 (1998) 69–94. [https://doi.org/10.1016/S0045-7825\(97\)00218-1](https://doi.org/10.1016/S0045-7825(97)00218-1).
- [41] F. Nosouhi Dehnavi, M. Safdari, K. Abrinia, A. Sheidaei, M. Baniassadi, Numerical study of the conductive liquid metal elastomeric composites, *Materials Today Communications*. 23 (2020) 100878. <https://doi.org/10.1016/j.mtcomm.2019.100878>.
- [42] An Introduction to Genetic Algorithms | The MIT Press, (n.d.). <https://mitpress.mit.edu/books/introduction-genetic-algorithms> (accessed September 26, 2020).
- [43] J. Cohoon, J. Kairo, J. Lienig, Evolutionary Algorithms for the Physical Design of VLSI Circuits, in: Springer, Berlin, Heidelberg, 2003: pp. 683–711. https://doi.org/10.1007/978-3-642-18965-4_27.